Data
Models
Inventories

PARIS

Process Attribution of Regional Emissions

GA 101081430, RIA

High-frequency N_2O observations uploaded to ICOS Portal

D5.1			
Delivery due date Annex I	M14 | February 2024		
Actual date of submission	M18 | June 2024		
Lead beneficiary: EMPA	Work package: 5	Nature: Data	Dissemination level: public
Responsible scientist	Stephan Henne		
Contributors	Stephan Henne, Empa		
Internal reviewers	Sylvia Walter, UU		
Version: 01			

Horizon Europe Cluster 5: Climate, energy and mobility
"This project has received funding from the European Union's Horizon Europe Research and Innovation programme under HORIZON-CL5-2022-D1-02 Grant Agreement No 101081430 - PARIS".

Table of content

1. Changes with respect to the DoA (Description of the Action)

No changes with respect to the DoA.

2. Dissemination and uptake

The N_2O observational data compiled for this deliverable will be used directly by the inverse modelling teams within PARIS WP5 and will be shared with the partner projects EYE-CLIMA and AVENGERS. The data were made publicly available on the ICON Carbon Portal following FAIR principles.

3. Short Summary of results

This data set combines historic and ongoing N_2O observations across Europe from several networks and individual institutions. The main purpose of the data set is to provide input to atmospheric inversion of N_2O fluxes. As such only observations from the highest inlet were considered at tall tower sites.

The data set comprises observations from traditional GC-ECD systems as well as modern laser spectroscopy instruments. In addition to continuous observations, flask observations from the NOAA network were included. A total of 50 time series from 43 observing sites are included covering the period 2005 to the end of January 2024. Of these sites 28 were reporting continuous observations in 2023, although some of these (ICOS NRT) remain preliminary at the time of compilation. The data and metadata items were brought to the same format including a common flagging system and reporting of uncertainties. Additional outlier flagging was applied and may be considered by the user for additional filtering. Original network flags were maintained. Different elements of measurement uncertainty are reported by different networks/institutions. Depending on availability, three different components of uncertainty were maintained in the data reflecting standard deviation of the ambient observation during the observation interval, repeatability of working standards and combined uncertainty. N_2O data are mostly reported on the WMO-X2006A calibration scale, with some exceptions reporting on the SIO-98 and SIO-16 scales. Due to possible temporal drifts between these scales, no correction was attempted. Hence, additional site-to-site bias correction (< 0.5 ppb) may be required when using the data in inverse modelling.

4. Evidence of accomplishment

Data are available on the ICOS Carbon Portal under the following doi: https://doi.org/10.18160/XQ9S-SXJ3.

4.1 Introduction | Background of the deliverable

Surface in-situ observations of greenhouse gases form the backbone of any inverse estimate of greenhouse gas fluxes to the atmosphere. The landscape of atmospheric N_2O observations in Europe was traditionally driven by individual research groups deploying instrumentation at a small number of sites within the continent. In addition, NOAA's flask sampling program included various European sites, both on the continent and remote baseline sites over the ocean.

During the European project InGOS an effort had been made to harmonize N_2O measurement techniques among several participants and report the data in a uniform format. However, observations after the end of InGOS were not collected/processed in the same way and were only available from individual PI's. With the advent of ICOS new N_2O observations became available through the ICOS Carbon Portal after 2017, following the strict ICOS data quality requirements. In contrast to traditional GC-ECD observations, ICOS requires laser spectroscopy instrumentation, achieving much better precision and measurement frequency. Similarly, several non-ICOS sites were equipped with laser-based instrumentation after 2017, but data were not collected in a uniform format. Within the EU project VERIFY further effort was undertaken to provide homogenized N_2O data set across European sites that could be used directly for inverse modelling of N_2O fluxes. This effort was renewed as part of PARIS and its partner projects AVENGERS and EYE-CLIMA and is documented as part of this deliverable report and resulting in an updated N_2O data collection readily available to all three consortia and the public through download from the ICOS Carbon Portal.

In contrast to the other major greenhouse gases CO_2 and CH_4, no such updated data collection was available at the start of the projects. For CO_2 and CH_4 so-called European Obspacks are annually collected by the ICOS ATC. For the 2024 updates and beyond, the ICOS ATC will start to include N_2O as well.

4.2 Scope of the deliverable

Consortia partners from PARIS, EYE-CLIMA and AVENGERS will use the data collected here as input to atmospheric inversions (PARIS milestone M20 and deliverable D5.2). For N_2O, surface in-situ data provide the only reliable atmospheric constraint for flux inversions. With this data collection, inverse N_2O emission estimates for western and central Europe will be feasible from 2005 onwards. However, data availability between 2012/2013 and the onset of ICOS and other observations after 2017 may limit the precision of such estimates during this period.

4.3 Content of the deliverable

4.3.1 Overview

This report briefly describes the data collection and processing process and gives additional information on provided data columns, metadata and specific data treatment.

Fig. 1 gives an overview of the sites from which N2O data was collected. A total of 50 time series from 43 observing sites covering the period 2005 to the end of January 2024 are included in the final product. 28 sites were reporting continuous observations in 2023. Table 1 clearly indicates the improvements in N2O data availability achieved in the last 5 years, which is mostly due to the efforts within the ICOS network and the availability of robust, laser-based measurement instrumentation.

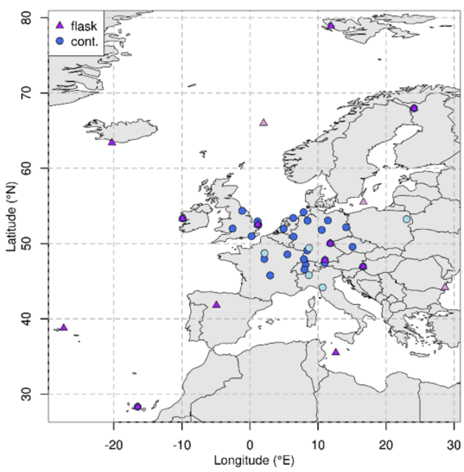

Fig. 1: Map of sites included in the present data collection. Blue circles continuous and purple triangles flask sampling observations. Light colors indicate sites which were not reporting observations in 2023 (continuous) and 2022 (flasks) anymore.

The spatial coverage of European N_2O observations remains sparse in Southern and Eastern Europe and most of Scandinavia, essentially limiting the capacity for inverse modelling to Western and Central Europe.

Table 1: Availability of N_2O observations at European site as included in compiled data set. Darker colors indicate greater availability. For continuous observations availability is given in percent (blue), for flask sampling availability is indicated as the number of flask pairs per year (purple).

ID	Type	Longitude	Latitude	Altitude	Inlet	2005	2006	2007	2008	2009	2010	2011	2012	2013	2014	2015	2016	2017	2018	2019	2020	2021	2022	2023
BIK	C	23.01	53.23	183	300	11	26	25	30	19	9													
BRM	C	8.18	47.19	797	212													63	75	86	99	96	97	97
BSD	C	-1.15	54.36	382	248													75	92	100	100	61		
CBW	C	4.93	51.97	0	207	62	80	68	85	36	81	69	70	72	75	82	66		94	39		24	44	44
CMN	C	10.68	44.17	2165	7				36	70	59	48	32	30	61	54	82	85						
GAT	C	11.44	53.07	69	341															70	96	95	97	81
GIF	C	2.15	48.71	160	7	38	41	82	62	67	78	84	76	59	85	43								
HEI	C	8.68	49.42	113	30	88	94	97	95	92	90	87	94	88	69									
HEL	C	7.88	54.18	43	110																36	98	25	96
HFD	C	0.23	50.98	158	100										86	100	89	55	84	97	87	98	97	89
HPB	C	11.02	47.80	934	131													81	89	96	95	92	90	87
HUN	C	16.63	46.95	248	96		31	31	45	25								74	73	70	75	64	76	70
IPR	C	8.64	45.81	210	16						20	71	54	66	61	60	70	85	39					
IZO	C	-16.50	28.31	2373	30			52	73	92	94	92	92	93	90	93	83						14	89
JFJ	C	7.99	46.55	3580	10	80	63	68	84	98	94	97	88	92	84	74	81	87	86	56	20	57	94	81
JUE	C	6.41	50.91	98	120															19	74	43	94	97
KIT	C	8.42	49.09	110	200															40	96	97	96	97
KRE	C	15.08	49.57	534	250														62	71		60	90	97
LIN	C	14.12	52.17	73	98														67	93	94	95	91	97
LUT	C	6.35	53.40	1	60		36	75	76	90	57	40	54	28	86	63	70		31	50	91	41	94	94
MHD	C	-9.90	53.33	8	10	80	78	85	83	87	89	89	88	88	90	87	84	91	76	88	85	86	76	81
OPE	C	5.50	48.56	390	120															20	49	94	73	91
OXK	C	11.81	50.03	1022	163		17	26	21	34	33	31	15	24	21					26	96	91	96	97
PAL	C	24.12	67.97	560	12																		65	88
PUY	C	2.97	45.77	1465	10						26	75	44	63						67	94	71	33	96
RGL	C	-2.54	52.00	207	90								66	85	98	72	94	93	93	98	97	88	91	95
SAC	C	2.14	48.72	160	100															86	96	97	95	88
SSL	C	7.92	47.90	1205	6	85	88	94	69	85	87	72	89	86	79	90	83	92	97	86		41	91	96
STE	C	8.46	53.04	29	252															41	97	97	94	94
TAC	C	1.14	52.52	64	100								36	94	98	92	97	83	91	92	88	84	86	76
TAC	C	1.14	52.52	64	185												31	86	95	96	98	96	93	80
TOH	C	10.54	51.81	801	147															14	98	90	97	91
TRN	C	2.11	47.96	131	180						73	71	24							51	83	96	94	91
WAO	C	1.12	52.95	31	10										12	76	87	81	87	15		43	90	83
ZSF	C	10.98	47.42	2656	3	91	83	77	82	85	49				59	74	89	88	94	98	50	91	72	97
AZR	F	-27.38	38.77	19	5	28	25	46	30	37	7	9	17	13	31	31	36	16	21	43	50	40	12	
BAL	F	17.22	55.35	3	25	61	85	95	99	97	82	46												
BSC	F	28.66	44.18	0	5	47	34	46	49	43	46	44	1											
CIB	F	-4.93	41.81	845	5					33	47	46	43	46	44	42	38	42	38	38	21	46	42	
HPB	F	11.02	47.80	985	5		34	46	48	47	46	42	46	45	47	50	48	47	44	49	45	49	50	
HUN	F	16.65	46.96	248	96	43	47	50	44	49	43	44	46	44	47	49	49	42	48	45	40	44	49	
ICE	F	-20.29	63.40	118	9	49	51	49	52	49	51	50	53	50	48	50	52	40	45	46	50	46	48	
IZO	F	-16.50	28.31	2373	5	35	39	47	47	42	45	48	47	48	49	51	51	53	48	51	47	51	48	
LMP	F	12.62	35.52	45	5		11	48	49	46	46	39	36	36	33	43	45	43	45	43	49	48	47	
MHD	F	-9.90	53.33	5	21	40	41	38	41	36	45	48	45	41	44	47	42	47	40	42	43	45	9	
OXK	F	11.81	50.03	1022	163		16	37	23	39	33	48	44	44	29	36	33	37	41	21		28	49	
PAL	F	24.12	67.97	565	5	44	39	50	48	48	49	48	46	40	49	49	50	46	47	49	38	50	50	
STM	F	2.00	66.00	0	5	81	97	89	100	91														
TAC	F	1.14	52.52	56	180										19	31	1							
ZEP	F	11.89	78.91	474	5	49	50	50	43	43	44	51	52	52	51	53	54	49	47	49	50	53	50	

4.3.2 Collection and dissemination

Data sources

The main data sources for this data collection were the existing ICOS, UK DECC and NOAA flask sampling networks. In addition, the data collection as carried out by INGOS and VERIFY were taken as starting point to identify any historical data sets. Some of these were available from the GAW world data center for greenhouse gases (WDCGG). Other data sets were requested directly from individual station PIs. Finally, the N2O observations from the Hungarian tall tower site (Hegyhátsál, HUN) were re-calibrated from 2017 onwards as part of the PARIS project (see also M17).

Data collection

Were available, data were downloaded from abovementioned sources. Additional, observations were requested from station PIs by email. Not all PIs were able to provide additional observations to those contained in previously published products either because observations were stopped altogether (e.g., IPR) or no people power was available to carry out required calibration/quality control. The latter may explain data gaps at some sites that are now part of ICOS but are lacking published observations prior to ICOS. An additional push to preserve this historic data was beyond the scope of the PARIS project but should be pursued in future activities.

Data provenance

Wherever raw data was taken from a public source, available under a permanent link (or DOI), these links/identifiers were maintained in the final product as part of the 'SOURCE URL' metadata item in the data header.

Data processing software

In order to bring all received/download data onto the same data format a dedicated software package, which was previously initiated for the project VERIFY, was extended and is publicly available (see https://gitlab.com/empa503/atmospheric-measurements/n2oobspack). In a first step, the tool ingests raw data as provided, renaming data columns and adding metadata from a metadata table where required. Three separate pieces of information were required from the raw data for each reporting time: the actual mole fraction of N_2O, a quality flag and an uncertainty estimate of the observation. Quality flags and the kind of uncertainty differed for different networks and data submitted by individual PIs. In addition, metadata was collected from the available data files themselves. If metadata was not available directly, it was collected and added 'manually'.

All continuous observations were aggregated to hourly values where needed.

Flagging

Since different data providers employ different flagging strategies, an attempt was made to harmonize these flagging systems. A somewhat simplified integer-based and additive flagging approach was chosen, with the individual flag values given in Table 2. These values are additive and with increasing value the data becomes less valid. The translation from original network flags to the collection flags were mostly deciding between valid (0), invalid (32) and questionable (2). Furthermore, ICOS near real time data, which did not go through manual quality control, was assigned a separate flag (1).

Table 2: Unified flagging system used in the data collection reported as 'CollectionFlag'. Additional flag values are derived as sums of the individual identifiers.

Flag value	Meaning
0	Generally valid observation
1	Near real time observation (no manual QC)
2	Questionable observation
4	Outlier detection
8	Large flask pair difference (only NOAA flasks)
32	Generally invalid observation

Two additional flags were assigned during the collection procedure. NOAA flask samples which are provided as dual-flask samples were averaged to provide a single value at each time. If differences between the two flask samples were large (>0.5 % of mean) an additional flag was assigned to these observations (see flagging).

Furthermore, an outlier detection algorithm was applied to all continuous observations. This algorithm employs the 'robust estimation of baseline signal' (REBS, Ruckstuhl et al., 2012) strategy to iteratively estimate a smooth baseline concentration and its uncertainty. For observations smaller than the baseline concentration minus three times the baseline uncertainty ($y < y_b - 3\sigma_b$) an additional outlier flag is set. This flag can be useful to exclude erroneous data but may also select observations impacted by intrusions of stratospheric air, which are more frequently observed at high-altitude sites. Such situations may still be discarded from the use in atmospheric inversions depending on whether or not the employed transport models are able to describe stratospheric intrusions correctly. If that is not the case, we still recommend excluding outlier flagged data at high-altitude sites.

In addition, to the unified data collection flag the data set contains the original network flags (column OriginalFlag) and a translation to the default ICOS flagging system (column Flag).

Calibration scale

Most of the collected data were already reported on the commonly used WMO-X2006A (NOAA2006A) scale (Hall et al., 2007). Exceptions were time series from the DECC network connected to AGAGE that report on the SIO-16 scale. Finally, some historic observations were also given on the SIO-98 scale (e.g., JFJ before 2015).

After re-evaluating available scale comparisons (NOAA round robin experiments[1] and sites with more than one time series on different scales like MHD), it was decided that an attempt to correct for potential offsets and biases in the calibration scales is currently not feasible. On the one hand, differences as obtained from the last round robin exercise revealed inter-lab differences of the order of 0.5 ppb even when reporting on the same scale. On the other hand, comparisons of co-located observations indicate a drift of inter-scale differences with time. Because of the snapshot character of the round robin experiments and the temporal drift, it seems to be impossible to apply a fixed scale correction at a given time.

As a result, calibration and scale biases in the order of 0.5 ppb can be expected to remain in the current data set and should be considered when using the observations in regional inversions (e.g., optimizing a constant site bias as part of the state vector).

Uncertainty reporting

Three different pieces of uncertainty are provided in the compiled data set depending on the availability of these in the original data:

1) Standard deviation of the observations during the averaging interval

This is mainly provided for the continuous, high-frequency, laser-based instruments, which evaluate this quantity from either high-frequency raw data or intermediate time averages (e.g., minute data). Note that, strictly speaking, the observed standard deviation is not a measure of measurement uncertainty but mostly reflects atmospheric variability, which is usually larger than measurement uncertainty. Nevertheless, the observed standard deviation may still be used as an indicator of model-data-mismatch uncertainty as required by inverse modelling systems.

[1] https://gml.noaa.gov/ccgg/wmorr/wmorr_results.php?rr=rr6&param=n2o

2) Repeatability of standard gas observations

Different networks provide a measure of difference between observed and expected standard gas measurements. It can be deemed as good measure of overall measurement uncertainty. Within ICOS this property is reported as short-term target bias (STTB), and we follow their nomenclature here. Within ICOS STTB is reported as the observed bias (positive/negative) from expected target gas concentrations. Others define it as the repeatability uncertainty of target observations, estimated as RMSE towards expected target concentrations.

3) Some networks provide a combined measurement uncertainty (e.g., NOAA flasks) that was estimated through individual quality assurance.

Merging data from different instruments

At several sites, more than one instrument was operated during certain overlap periods. In addition, some of the received historical data overlapped with data already incorporated into ICOS. In order to provide a single time series per site, which can be directly used in inverse modelling, we merged all continuous data streams from an individual site and inlet height. Flask data were not merged with continuous data were both were available from the same location. In the merge priority was given to ICOS data over historical data and to laser-based instruments over GC instruments. The merge was done applied on an hourly basis potentially leading to a gap filling of the primary instrument when the secondary instrument was available. The data origin for each hourly value is reported as a separate column in each data file.

Output format

Data is provided as individual files per sites and measurement type (flaks/continuous) using ASCII format and character separated values. Header lines are identified by hash (#) characters and metadata fields are detailed below. Data columns are listed in Table 3. The format follows ICOS standards and, as such, a data preview is available along with the data on the ICOS Carbon Portal.

Table 3: Data columns provided in ASCII presentation of N_2O data files.

Column	Comment
Column	Comment
Site	3-letter station abbreviation
Year, Month, Day, Hour, Minute	Date/time information of observation. All times are UTC and specify the beginning of the averaging period.
DecimalDate	Date/time information provided as year with decimal placed giving time within year.
n2o	N2O mole fractions in units nmol mol^{-1}.
Stdev	Standard deviation of observation (details see uncertainty reporting)
NbPoints	Number of original (or intermediate) observations used for averaging and standard deviation.
Flag	ICOS-like data quality flag. Translated from CollectionFlag.
CollectionFlag	Unified collection data quality flag (details see flagging).
OriginalFlag	Original data quality flag provided by network/PI.
STTB	Target bias/uncertainty (repeatability) (details see uncertainty reporting) in units nmol mol^{-1}.
Unc_n2o	Originally reported combined measurement uncertainty in units nmol mol^{-1}.
Scale	Calibration scale given as an integer identifier referring to metadata item 'MEASUREMENT SCALE'.

Longitude	Longitude of observation in units degrees East.
Latitude	Latitude of observation in units degrees North.
Intake_height	Height above ground (units meters) of sample inlet.
Origin	String identifying source of data (network/instrument name).

Metadata items

Next to the metadata available on the Carbon Portal each provided data file contains its own set of metadata items facilitating the proper use of the data. Each metadata item consists of a name and value pair given as single header line. Next to items describing the data, a 'data policy', 'fair use' and 'warning' statement is provided. These statements follow the projects' generally open data policy.

4.3.3 Time series inter-comparison

Next to the quality control performed by each station PI or network, we conducted additional validation tests by inter-comparing each obtained time-series to data from neighboring sites. Inconsistencies in general observation levels and periods of questionable deviations between sites should be identifiable in this way. A comparison to neighboring data can never be an absolute assurance of the current data quality as various factors may still impact each local observation. These include the local emission and flow situation, with sites closer to large N_2O emissions (e.g., within intensely managed agricultural areas) and situated in less well-ventilated regions (e.g., continental vs. coastal) experiencing generally larger mole fractions and variability. Furthermore, site altitude may render the direct inter-comparison, with high-altitude sites generally experiencing lower mole fractions than boundary layer sites. Finally, larger-scale spatial gradients may make the comparison more complicated. This includes a general north-south gradient as expected for the hemispheric baseline as well as a general east-west gradient expected from the dominating westerly flow, bringing relatively clean air into Europe and increasing accumulation when moving eastward. We tried to increase the comparability by estimating monthly mean baseline values for each observation site and measurement type (flask vs. continuous). For continuous observations the REBS method was applied to extract baseline mole fractions before calculating monthly means. For flaks samples it was assumed that these are mostly taken during baseline conditions and direct averaging to monthly mean mole fractions was applied. For each site, the four closest neighboring time series were evaluated. Average bias and RMSE for monthly time series were calculated as an objective indicator of inter-comparability. For sites with continuous and flaks sampling this contained the mutual series.

Here, we show examples of this inter-comparison for example sites representative of different European areas. All further comparisons did not reveal any other discrepancies between the individual observations, highlighting the very good quality and usability of the compiled data set.

Fig. 2 shows the comparison for the western in-flow region from the North Atlantic, includes the sites Azores, Mace Head and Izana and spans over the full period of the data collection. At both Mace Head and Izana flask and continuous observations were available during most of the period. The largest bias for this set of five time series can be seen between the continuous measurements at Mace Head and the flaks sampling at Azores (0.5 nmol mol^{-1}). A similar bias also exists between the flaks and continuous data at Mace Head and may be cause by both sampling strategy and calibration scale differences. Note that for the most recent years this bias almost disappeared.

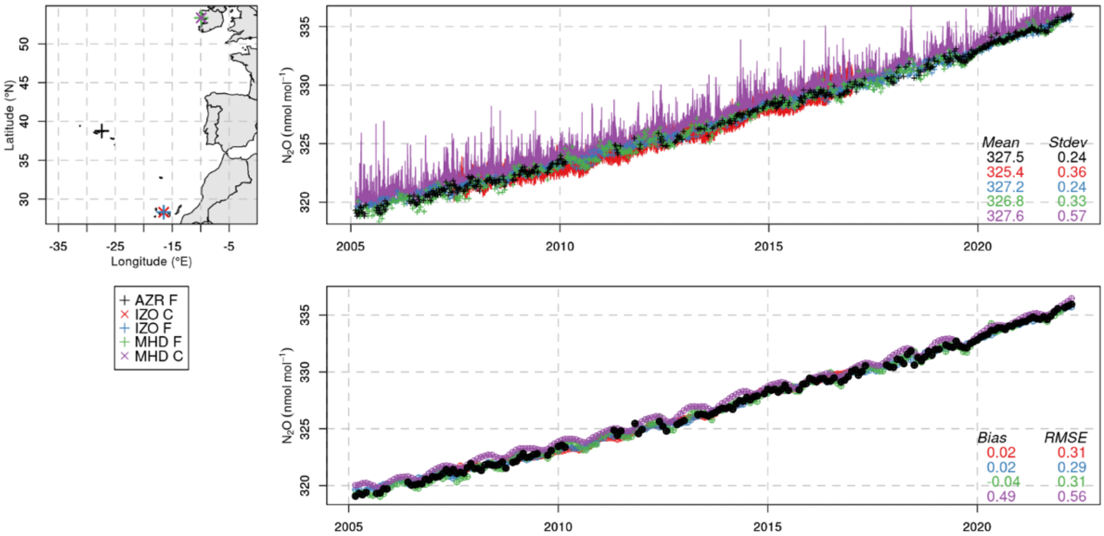

Fig. 2: N_2O time series of the flaks sampling observations on the Azores (AZR, black plus signs) and at neighboring sites. The top panel gives hourly and individual flask observations, respectively. Mean and standard deviation are applied over entire of each time series. The lower panel shows monthly mean mole fractions. Bias and RMSE are calculated from the monthly data with respect to the reference time series at AZR. All number referring to mole fractions in units nmol mol^{-1}.

Another example is given in Fig. 3 where data from the UK DECC network are compared. Overall biases and RMSE between monthly baselines means of the sites are all well below 0.5 nmol mol^{-1}. Different pollution levels are indicated by the overall standard deviation, with more polluted sites showing larger standard deviations and also a tendency to larger mean baseline mole fractions. The latter most likely related to shortcomings in the baseline estimation method that are more pronounced for more polluted sites with rare occurrence of real baseline levels.

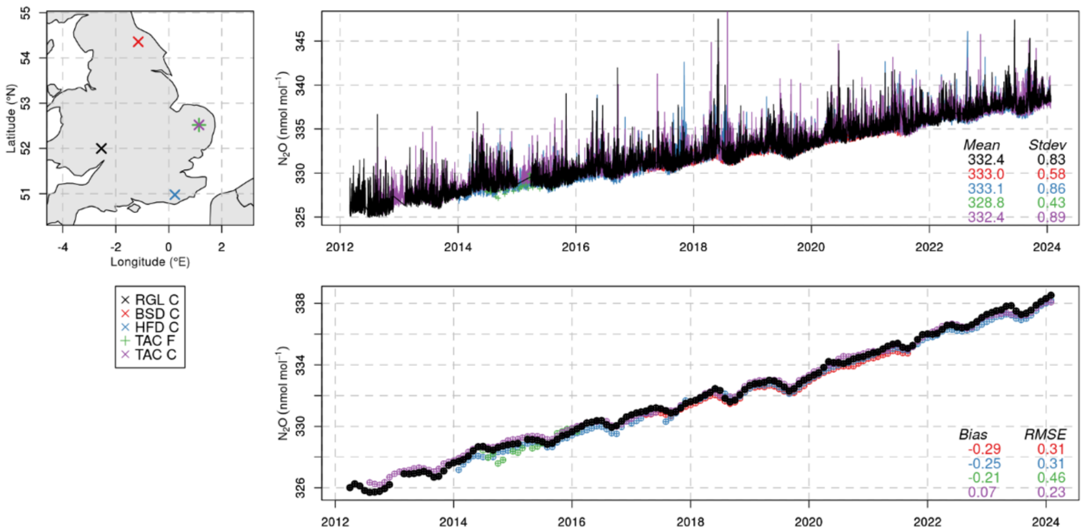

Fig. 3: N_2O time series of the continuous observations at Ridge Hill tall tower (RGL, black lines) and at neighboring sites. See Fig for further details.

An extended N_2O time series is also available from the tall tower site Cabauw, Fig. 4. Similar to the UK DECC network biases an RMSE with neighboring sites remain small. The German site on the island of Helgoland, HEL, shows the largest deviation with a mean bias of -0.6 nmol mol^{-1}. If the latter can be attributed to measurement bias or the island location of the site remains unclear.

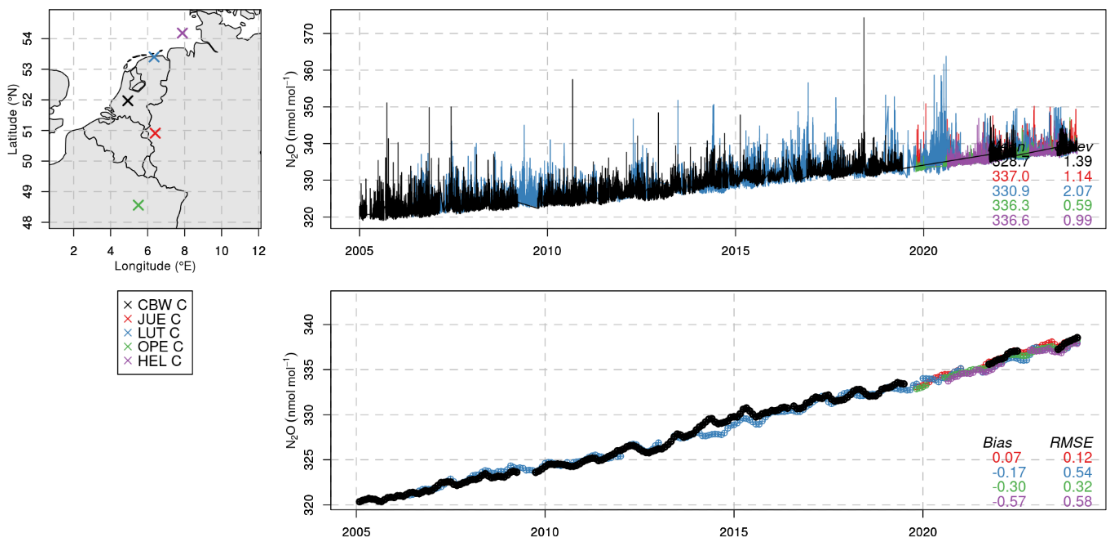

Fig. 4: N_2O time series of the continuous observations at Cabauw tall tower (CBW, black lines) and at neighboring sites. See Fig for further details.

Fig. 5 compares the more continental sites situated in northeastern Germany. These sites are characterised by relatively large pollution episodes as seen by the standard deviation of the observations. Nevertheless, biases and RMSE between the sites remain small. Similarly, the sites in southeastern Germany show very little deviations from each other even when considering the long time series of Ochsenkopf and Hohenpeissenberg (Fig. 6).

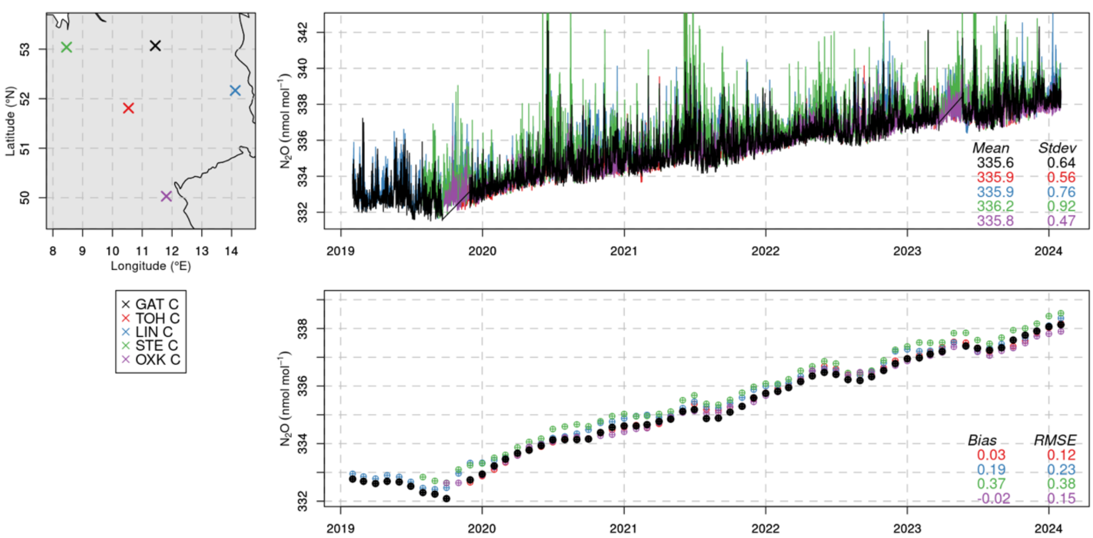

Fig. 5: N_2O time series of the continuous observations at Gatow tall tower (GAT, black lines) and at neighboring sites. See Fig. 2 for further details.

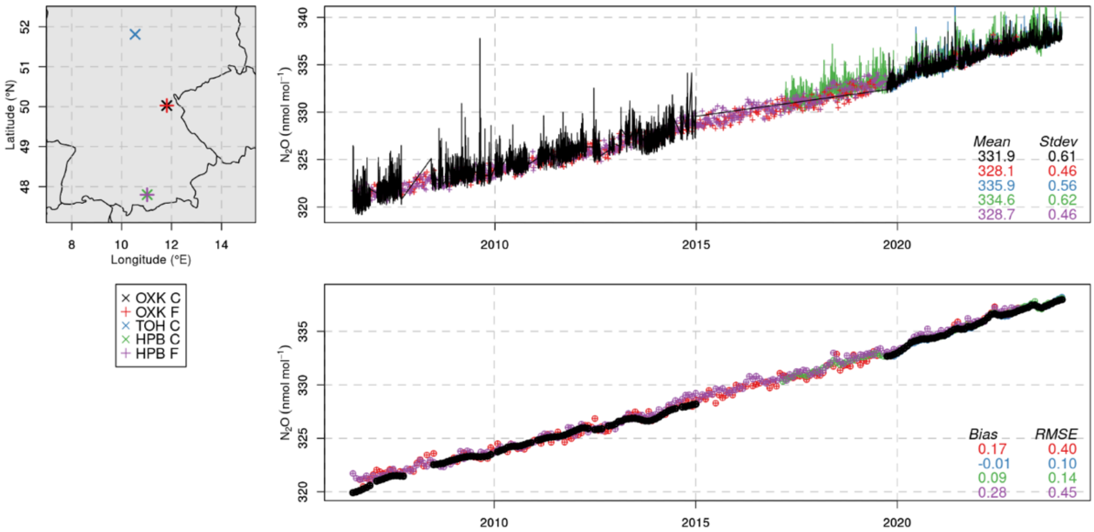

Fig. 6: N_2O time series of the continuous observations at Ochsenkopf tall tower (OXK, black lines) and at neighboring sites. See Fig. 2 for further details.

However, large biases are apparent from the comparison of the (pre-ICOS) observations at Ispra (IPR) and other sites in the Alpine area Fig. 7. The pre-ICOS time series from IPR is the only one for which a bias of this magnitude (2 nmol mol^{-1}) was detected. It cannot be ruled out that this bias is purely due to local factor impacting these measurements (valley location, strong local fluxes, low measurement height above ground). Still, this time series should only be used with caution in inverse modelling as these local factors may not be well represented in any atmospheric transport model and, hence, induce biases in regional flux estimates.

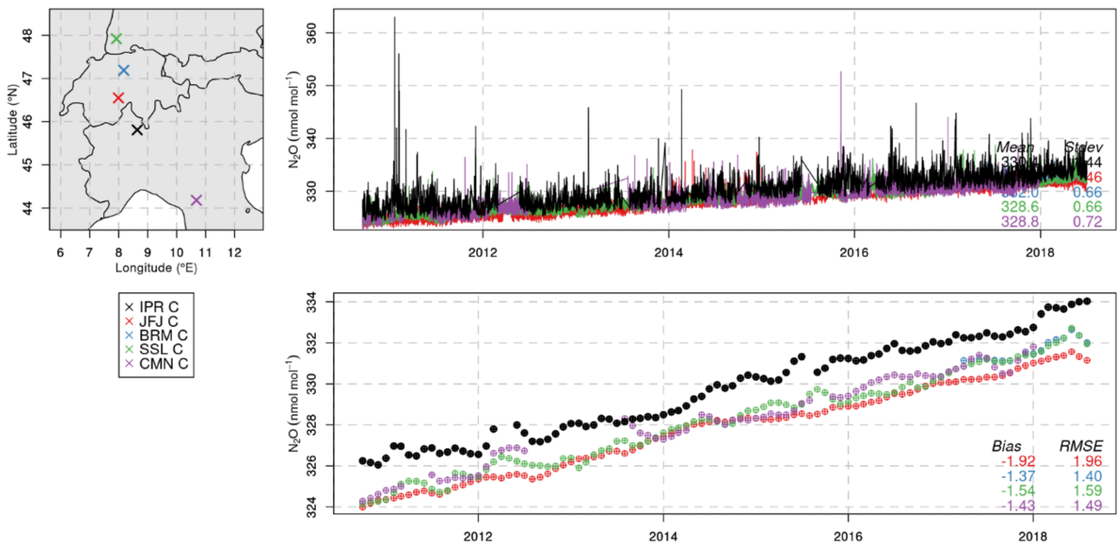

Fig. 7: N_2O time series of the continuous observations at Ispra (pre-ICOS) (IPR, black lines) and at neighboring sites. See Fig. 2 for further details.

Observations from easternmost sites in the collection are compared in Fig. The observations in Hungary (HUN) are characterised by very large variability, indicating strong regional sources and more continental dispersion conditions. However, the estimated baseline for HUN compares very well with those of neighboring sites, again with absolute biases remaining below 0.5 nmol mol^{-1}.

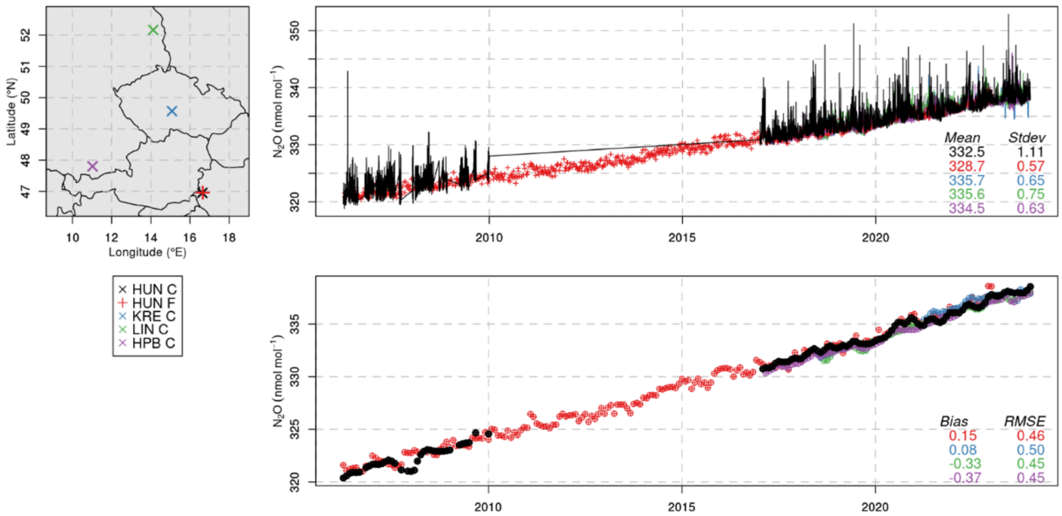

Fig. 8: N_2O time series of the continuous observations at Hegyhátsál tall tower (HUN, black lines) and at neighboring sites. See Fig. 2 for further details.

4.4 Conclusion and possible impact

This deliverable provides a description of the harmonised N_2O surface observation package that is intended for use in inverse modelling of N_2O fluxes across Europe for the period 2005 to 2023. The data collection was uploaded the ICOS Carbon Portal and is publicly findable and accessible.

Next to data format harmonisation, additional quality control was achieved by site-by-site data comparison. No major issues were identified illustrating the general high quality of the provided time-series. An exception is given by the (pre-ICOS) observations from Ispra (IPR), which seem to be impacted by local factors that will need to be sufficiently captured by an atmospheric transport model before the data should be used in inverse modelling. For all other sites, it is still recommended to consider site biases as part of the state vector in any inverse modelling attempt. Such bias are in general not expected be larger 0.5 nmol mol^{-1}.

The software package created for the data collection can be adjusted without large efforts to incorporate new data submissions/publications from the individual networks to compile updated versions of this collection. This may be necessary if no other European N_2O data collection (i.e., European obspack by ICOS ATC) becomes available before an update is required by the inverse modelling groups in PARIS, AVENGERS or EYE-CLIMA.

4.5 References

Hall, B. D., Dutton, G. S., and Elkins, J. W.: The NOAA nitrous oxide standard scale for atmospheric observations, J. Geophys. Res., 112, doi: 10.1029/2006JD007954, 2007.

Ruckstuhl, A. F., Henne, S., Reimann, S., Steinbacher, M., Vollmer, M. K., O'Doherty, S., Buchmann, B., and Hueglin, C.: Robust extraction of baseline signal of atmospheric trace species using local regression, Atmos. Meas. Tech., 5, 2613-2624, doi: 10.5194/amt-5-2613-2012, 2012.

5. History of the document

Version	Author(s)	Date	Changes
	Stephan Henne	2024-04-01	First draft
	Stephan Henne	2024-05-30	Close to final report
	Stephan Henne	2024-06-27	Minor corrections
	Sylvia Walter	2024-06-27	Minor corrections, formatting and submission